Supplementary Information for

Direct Evidence for Solid-Like Hydrogen in a Nanoporous Carbon Hydrogen Storage Material at Supercritical Temperatures

Valeska P. Ting, Anibal J. Ramirez-Cuesta, Nuno Bimbo, Jessica E. Sharpe, Antonio Noguera-Diaz, Volker Presser, Svemir Rudic, Timothy J. Mays

Correspondence to: v.ting@bath.ac.uk

This PDF file includes:

Materials and Methods

Characterization of carbon reference material

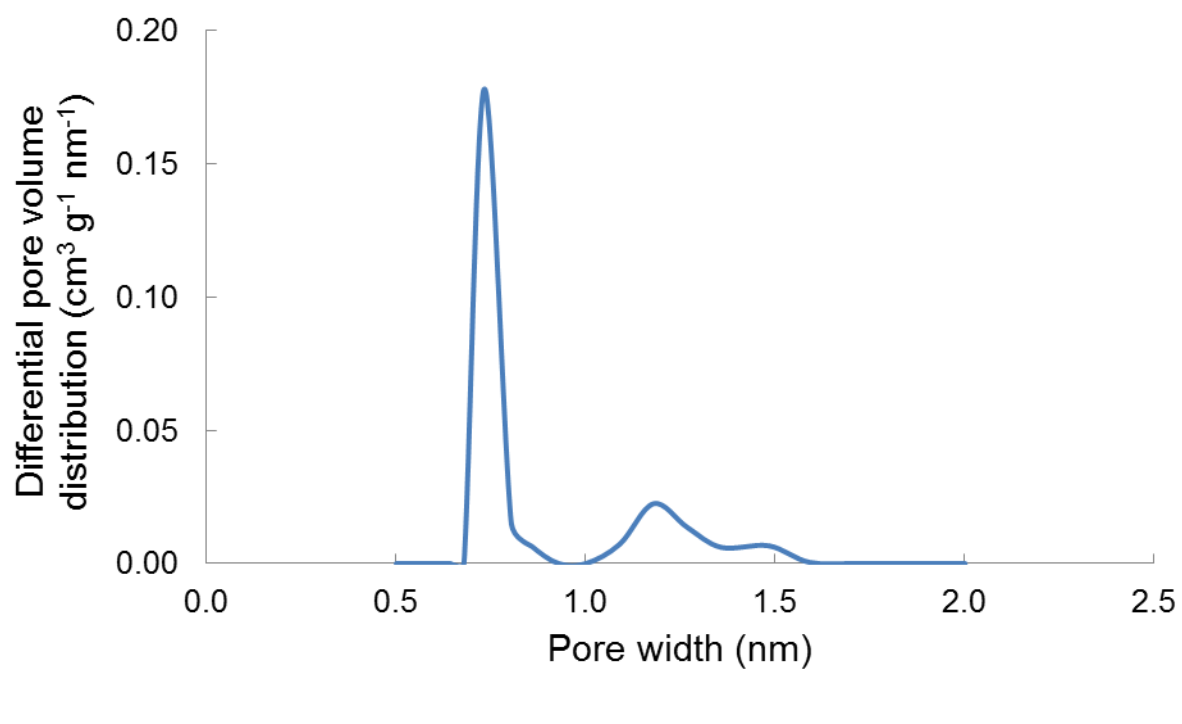

Fig. S1. Differential pore size distribution for the TE7 beads determined from density functional theory analysis of N_2 sorption at 77 K measured using a Micromeritics ASAP 2020 volumetric adsorption analyzer. The mean micropore width from Dubinin-Radushkevich analysis is ~0.7 nm.

Modeling the excess H_2 uptake to estimate the adsorbed H_2 density

Excess isotherms for the MAST TE7 carbon beads were analyzed and modelled using a modification of our previously reported methodology. [19,20] This modification consists of distinguishing between excess, absolute and total masses of adsorbed H_2 in the pore. The absolute corresponds to the amount of densified adsorbed H_2, with the total uptake comprising of the absolute as well as the bulk quantity of the gas within the pore. The model includes an adsorbate volume, (which is not necessarily equal to the pore volume), which represents the volume occupied by an adsorbed H_2 phase with a higher density than the bulk H_2. A fractional filling term, which represents the the ratio between the adsorbate volume and pore volume ($\theta_A = V_A/V_P$) is modelled using a Type I isotherm. The excess isotherm is fitted using (1) and with the fitted parameters from the excess, we can determine the absolute (2) and the total (3) isotherm.

$$m_E = (\rho_A - \rho_B)\theta_A V_P \quad (1)$$

$$m_A = \rho_A \theta_A V_P = m_E + \rho_B \theta_A V_P \quad (2)$$

$$m_P = \rho_A \theta_A V_P + \rho_B V_P (1 - \theta_A) = m_E + \rho_B V_P \quad (3)$$

In equations (1), (2) and (3), m_E, m_A and m_P are the excess, the absolute and the total adsorbed amounts in wt.%, respectively. The densities ρ_A and ρ_B are the adsorbate and bulk density, respectively, in kg m^{-3}. The fractional filling is a ratio of the adsorbed and pore volume V_P and it is modelled using a Type I equation.

The Type I isotherm used in the analysis was the Tóth[21] (a variation of the Langmuir that account for adsorption heterogeneity), which according to our previous studies, resulted in the best fit to the experimental data. The parameters in the fit (see Fig. S2) are ρ_A (in

kg m^{-3}), b (in MPa^{-1}), c (dimensionless) and V_p (in cm^3 g^{-1}), with An (n = 1, 2, 3, 4) being the parameters from the rational function approximation for the compressibility factor Z of the Leachman equation of state for H_2[1] as a function of pressure and *Temp* being the temperature in K. The density of the adsorbate comes from the fitting and is ρ_A, b and c are the Tóth affinity and heterogeneity parameters respectively and V_P is the specific (open) pore volume. The absolute amount (2) represents the adsorbate in the pore with a higher density than the bulk.

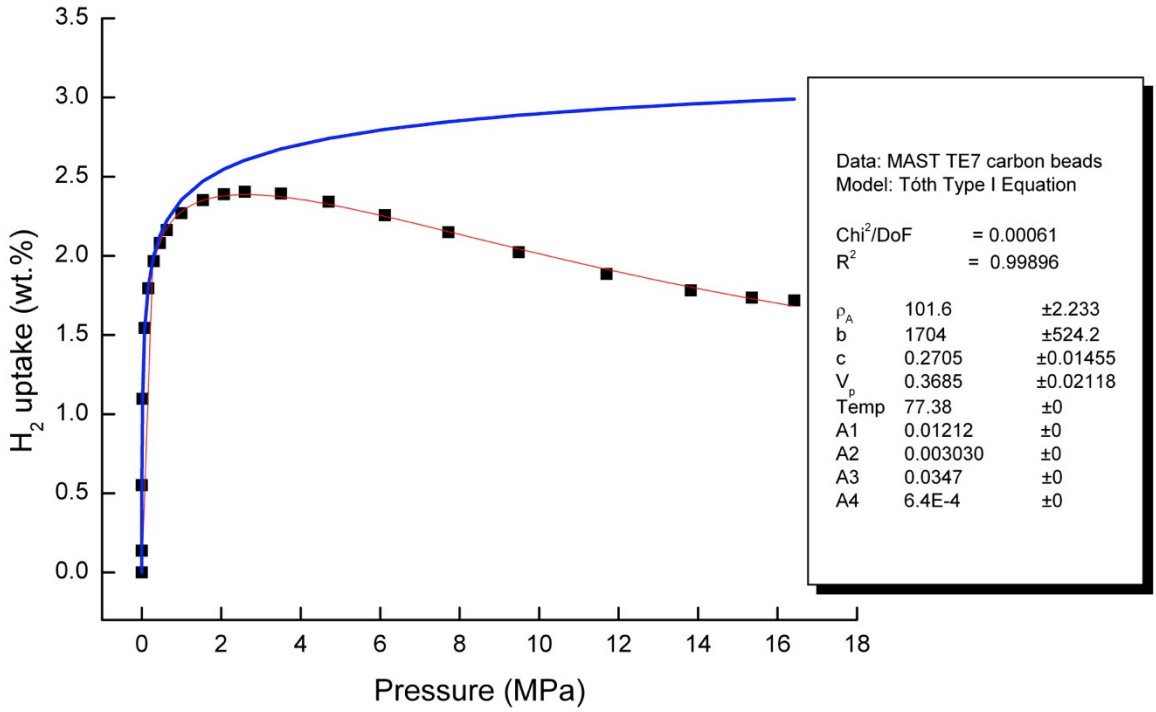

Fig. S2. Excess H_2 uptake as a function of pressure (up to 17 MPa) for MAST Carbon TE7 activated carbon beads obtained from a Sieverts-type volumetric gas dosing analyzer (Hiden Isochema HTP-1) (black squares). The excess isotherm was fit (red line) using (1) with the Tóth as the Type I equation for the absolute isotherm. Least-squares best fit parameters from the fit, and their standard errors, are displayed in the legend. The blue line indicates the

absolute amount adsorbed in wt.%, as calculated using the parameters from the fit and (2), and results in an estimated density of the adsorbed H_2 phase (ρ_A) of 101 ± 2 kg m^{-3}.

As a comparison, hydrogen excess isotherms on AX-21 modelled assuming a constant density of adsorbate resulted in calculated adsorbate densities ranging from ~90 kg m^{-3} at 90 K to ~71 kg m^{-3} at 120 K. [42]

Evidence for solid-like hydrogen

Elastic line: Dense phases of hydrogen will show an elastic peak contribution at ~0 meV. See the below backgound-subtracted spectrum from bulk solid normal hydrogen at 10 K. Note that at 30 K (gaseous hydrogen) the elastic peak is absent.

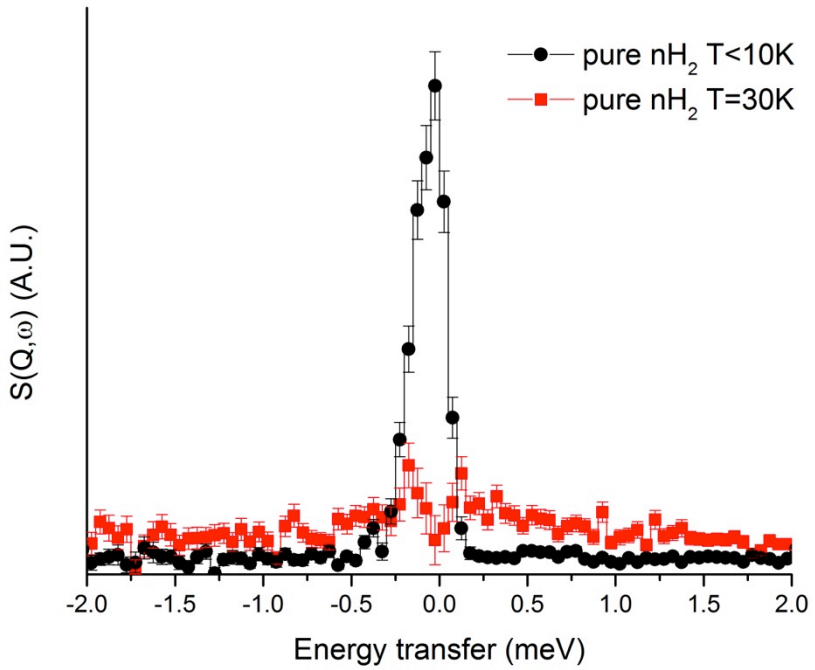

Fig S3: Spectra of the elastic contribution from bulk normal H_2 at the elastic line at $T <$ 10 K (solid), showing a FWHM of 0.23 meV (achieved using an annular sample can with a thickness of 0.1 mm, to minimize multiple scattering effects) and at T = 30 K with the background subtracted. Note that there is no elastic peak present for bulk hydrogen at 30 K.

While both solid and dense liquid phases will show an elastic contribution, the elastic line from a liquid will be typically broadened due to quasielastic interactions. At low loading (0.016 MPa H_2), the full-width at half-maximum of the elastic peak (~0.3 meV) from the hydrogen in our carbon sample approximated the instrumental peak resolution, indicating that all of hydrogen present had limited mobility.

Note: The excess width in the elastic line for the sample is a result of self-shielding and multiple scattering effects from the large (>10 cm^3) amount of sample in the beam and thick walled-high pressure sample cell, which have a large effect on lower energy peaks.

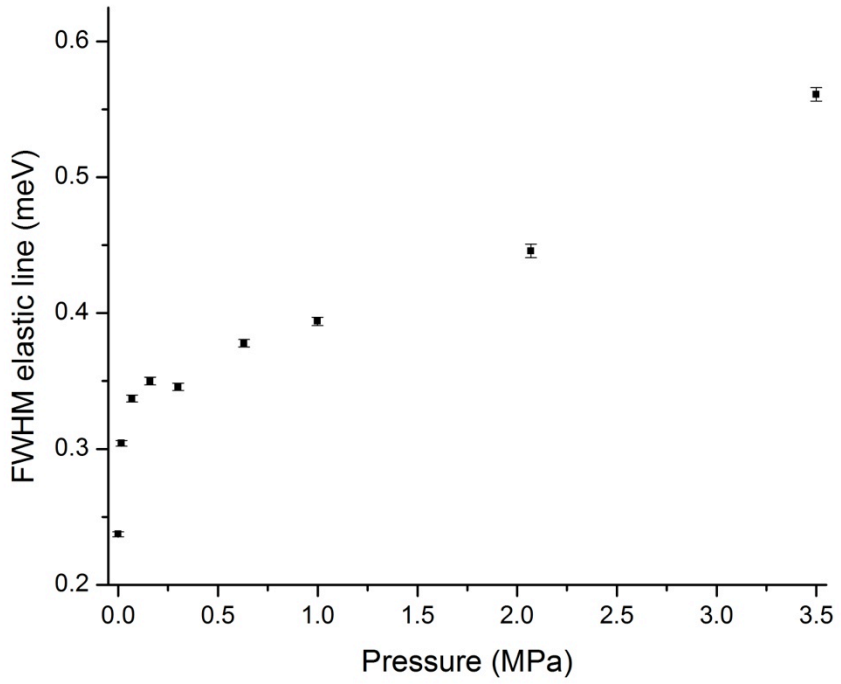

Fig S4: Evolution of the full width at half maximum (FWHM) of the elastic line from the background-subtracted sample at 77 K fitted with a Gaussian peak shape, as a function of normal H_2 pressure. Error bars represent the errors in the fitting parameters using a Levenberg-Marquardt algorithm. The first point (0 MPa, corresponding to the elastic line from the empty cell at 77 K) is included for comparison.

Rotor line: Unlike the study by Egelstaff [43] on the rotational transitions seen for solid and liquid hydrogen using cold neutrons and energy gain or the energy gain study by Fitzgerald *et al*. of a single H_2 molecule trapped in the octahedral interstice in solid C_{60}, [44] TOSCA uses thermal neutrons and tracks energy loss. In a typical spectrum for liquid hydrogen on TOSCA, the rotational line for liquid hydrogen is lost in the large recoil signal (Fig. S3 from the ISIS INS database, http://wwwisis2.isis.rl.ac.uk/INSdatabase/Theindex.asp, accessed November 2013).

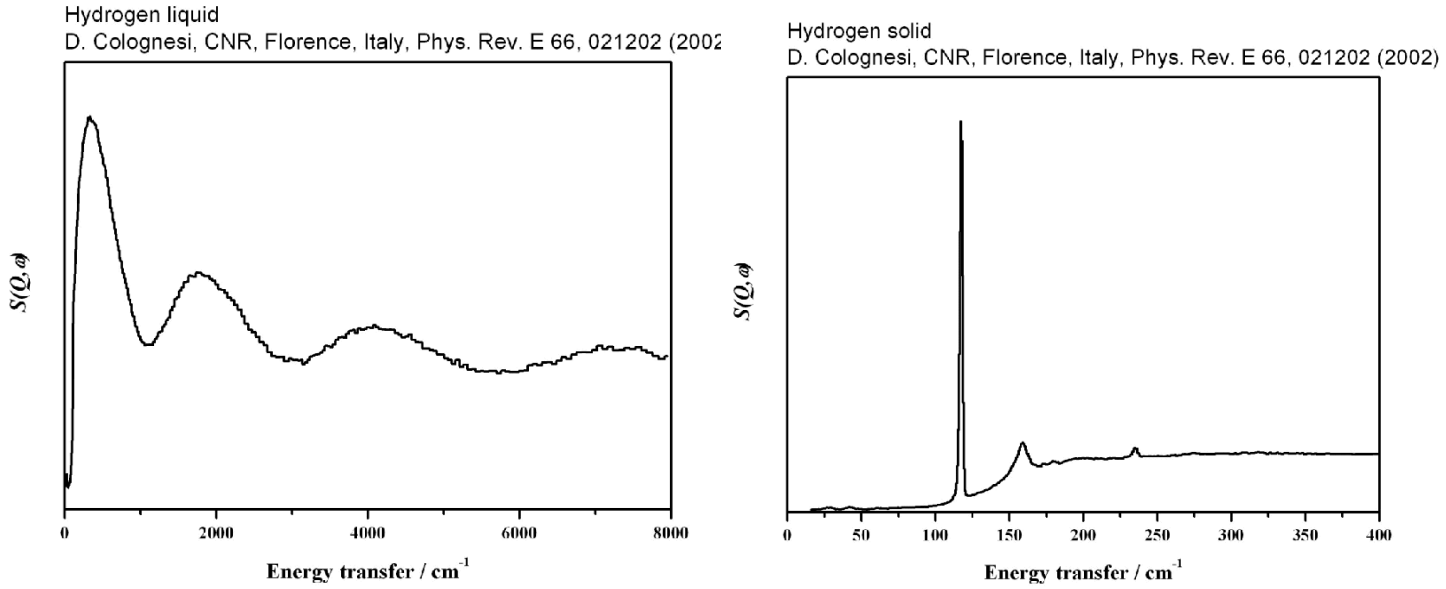

Fig. S5. INS energy loss spectra collected with thermal neutrons on (left) liquid *para*-H_2 (after can subtraction) at T = 17.2 K and P = 0.43 bar [45] and (right) solid H_2 at 12.2 K and P = 0.43 bar [46] showing the rotor line for *para*-H_2 at 14.7 meV (= 118 cm^{-1}).

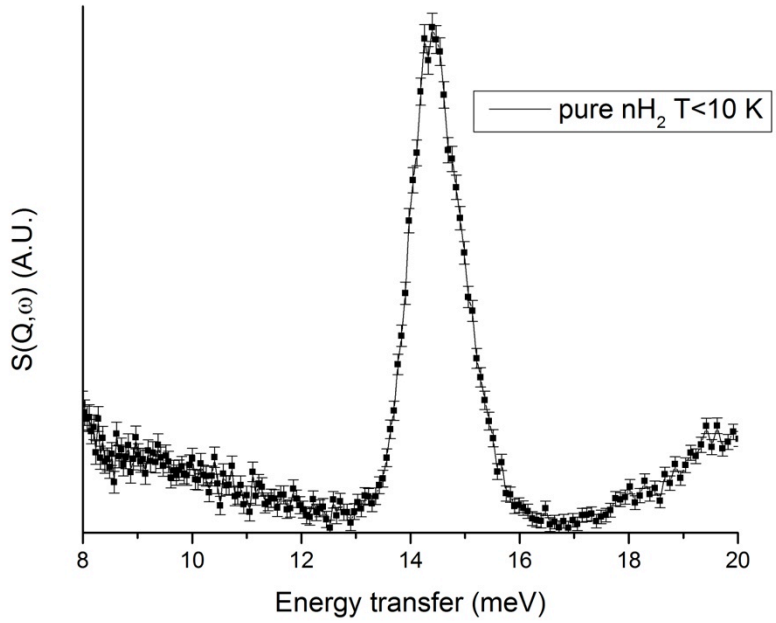

Fig S6: Spectrum of pure normal H_2 at $T < 10$ K (solid), showing the width of the rotational line, from Colognesi, D. *et al*. *Phys*. *Rev*. *B* (2007) [18]

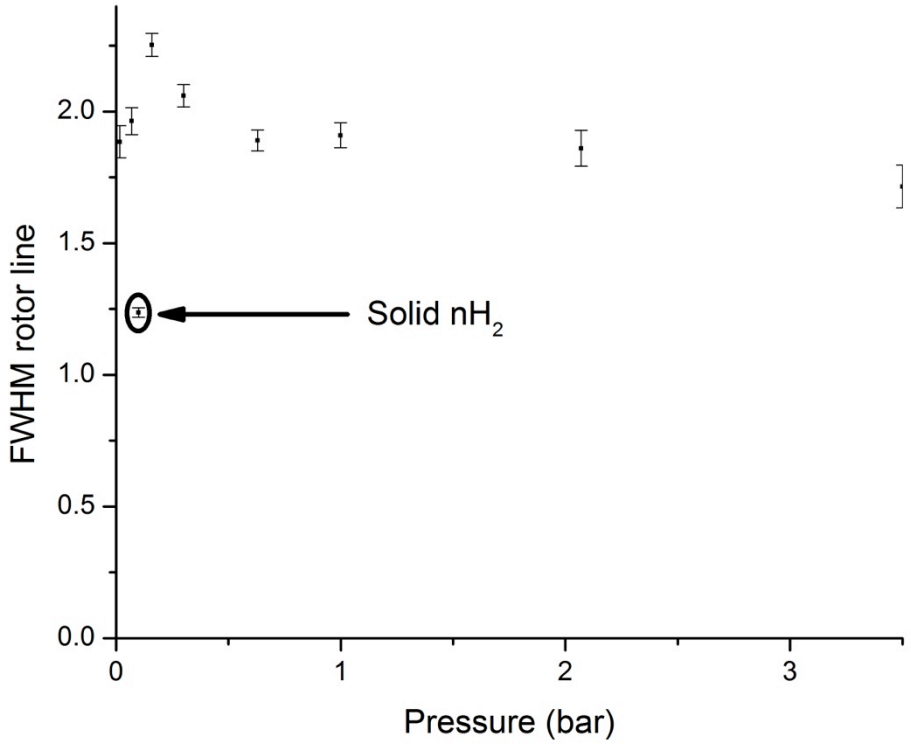

Fig S7: The evolution of the FWHM of the normal H_2 rotor line (~14.7 meV) as function of normal H_2 pressure at 77 K. The point highlighted by the circle corresponds to the width of the rotor line for pure normal H_2 solid (extracted from Colognesi *et al*. *Phys*. *Rev*. *B* (2007)[18]).

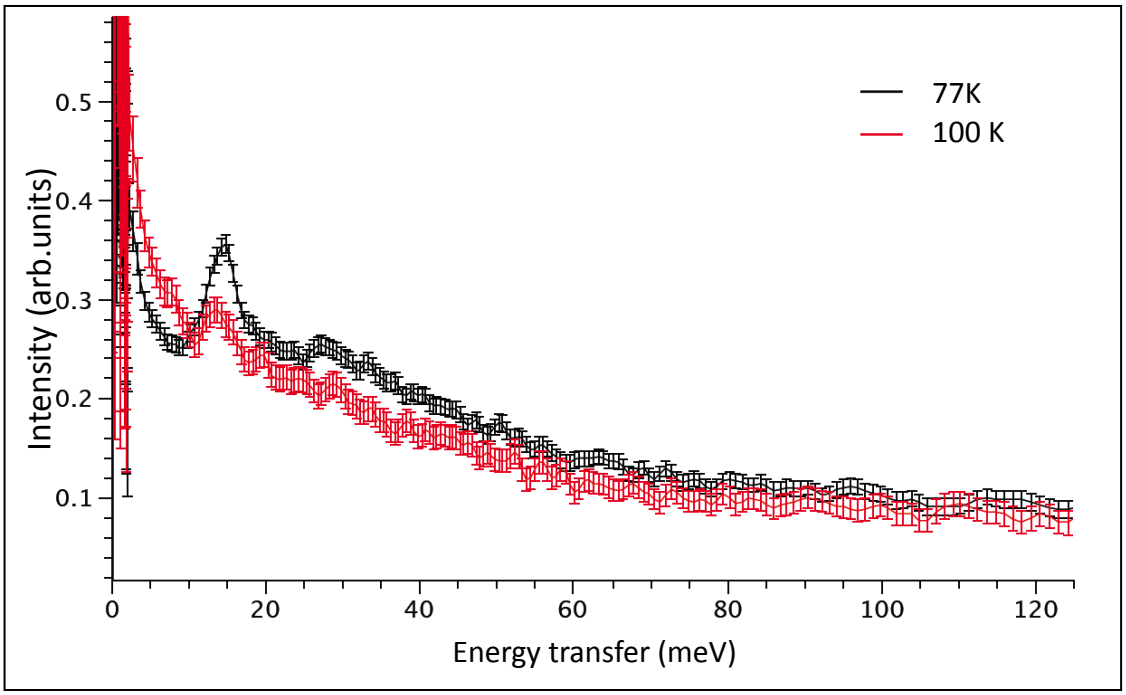

Fig. S8. Background-subtracted INS data from 0.0016 MPa H_2 at 77 K (black) and 100 K (red), showing the persistence of the 14.7 meV rotor line at 100 K. The sample was evacuated and dosed with 0.0016 MPa H_2 and a spectrum was recorded for 700 μA h at 100 K.

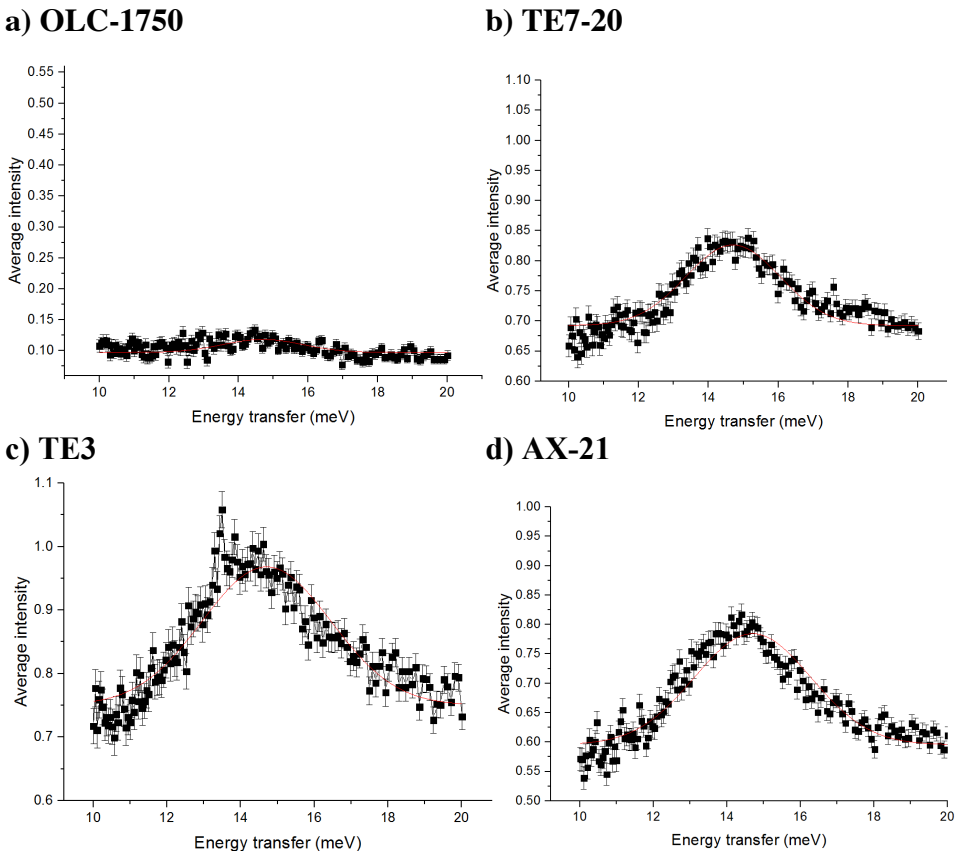

Fig. S9. Background-subtracted INS data from 0.1 MPa H_2 at 77 K from samples of a) OLC-1750 onion-like carbon, b) TE7_20 carbon from MAST Carbon, d) TE3 carbon from MAST Carbon and d) AX-21 activated carbon from Anderson Development Company, showing the existence of the 14.7 meV rotor line for the samples with pore diameters in the range ~6-8 A (samples b, c, and d). The OLC-1750 has very low micropore volume (see Table S3) and thus has no noticable peak in the 14.7 meV region. The samples were evacuated and dosed with 0.1 MPa H_2 and a spectrum was recorded for 700 μA h.

Comparison of INS integrated intensities and the volumetric excess H_2 uptake

Table S1: H_2 uptake with pressure, as measured on Hiden Isochema HTP-1 volumetric sorption apparatus.

H_2 dosing pressure for volumetric measurements (MPa)	Gibbs excess from gas sorption measurements (μmol)	Hydrogen uptake (wt%, dry carbon basis)
0	0	0
0.002	384	0.54
0.017	778	1.10
0.071	1100	1.56
0.167	1280	1.81
0.300	1394	1.97
0.457	1470	2.08
0.630	1521	2.15
1.000	1582	2.24
1.542	1616	2.28
2.071	1621	2.29
2.593	1607	2.27
3.505	1561	2.21

Table S2: Integrated intensity under the elastic line (–2 meV to 2 meV) with pressure, from the INS spectra up to ~3.5 MPa.

H_2 dosing pressure for INS measurements (MPa)	Integrated intensity under elastic line, background subtracted (arb. units)	Scaled integrated intensity under elastic line (wt%)
0	0.000	0.00
0.016	0.234	1.16
0.074	0.319	1.58
0.168	0.370	1.83
0.300	0.403	2.00
0.630	0.432	2.15
0.998	0.451	2.24
2.071	0.462	2.29
3.500	0.508	2.52

Table S3

Integrated area under the 14.7 meV rotor line from INS of the materials shown in Fig S9 (0.1 MPa H_2 at 77 K, background subtracted) fit with a Gaussian peak shape, and some structural characteristics of the materials, from volumetric N_2 sorption analysis at 77 K. Micropore volume was determined using Dubinin-Radushkevich model, and pore size distributions were estimated using a DFT slit pore model.

Material:	14.7 meV area peak (Gaussian):	BET (m^2 g^{-1})	Total pore volume (cm^3 g^{-1})	Micropore volume (DR) (cm^3 g^{-1})	Pore diameters (Å) (DFT, N_2, slit)
TE3	0.9561 ± 0.0742	1567 ± 21	1.24	0.73	5, 5.9, 8.3, 12 and 15
OLC-1750	0.0605 ± 0.0109	321 ± 0.66	1.29	0.13	11, 35, 94, 187, 334, 506, 687 and 855
AX-21	0.4533 ± 0.0243	2524 ± 47	1.82	1.97	5, 5.9, 8.3, 12, 16, 21
TE7_20	0.7510 ± 0.0436	1234 ± 7	1.33	0.52	6.8, 8.5, 12 and 15

Full reference list

1. Leachman, J. W.; Jacobsen, R. T.; Penoncello, S. G.; Lemmon, E. W., Fundamental Equations of State for Parahydrogen, Normal Hydrogen, and Orthohydrogen. *J. Phys. Chem. Ref. Data* 2009, 38, 721-748.
2. Datchi, F.; Loubeyre, P.; Letoullec, R., Extended and Accurate Determination of the Melting Curves of Argon, Helium, Ice (H_2O) and Hydrogen (H_2). *Phys. Rev. B* 2000, 61, 6535-6546.
3. Deemyad, S.; Silvera, I. F., Melting Line of Hydrogen at High Pressures. *Phys. Rev. Lett.* 2008, 100, 155701.
4. Schlapbach, L.; Zuttel, A., Hydrogen-Storage Materials for Mobile Applications. *Nature* 2001, 414, 353-358.
5. Van Den Berg, A. W. C.; Arean, C. O., Materials for Hydrogen Storage: Current Research Trends and Perspectives. *Chem. Commun.* 2008, 668-681.
6. Rouquerol, J.; Avnir, D.; Fairbridge, C. W.; Everett, D. H.; Haynes, J. H.; Pernicone, N.; Ramsay, J. D. F.; Sing, K. S. W.; Unger, K. K., Recommendations for the Characterization of Porous Solids. *Pure Appl. Chem.* 1994, 66, 1739-1758.
7. Broom, D. P., Hydrogen Storage Materials: the Characterisation of their Storage Properties. Springer Science & Business Media: 2011.
8. Züttel, A.; Sudan, P.; Mauron, P.; Wenger, P., Model for the Hydrogen Adsorption on Carbon Nanostructures. *Appl. Phys. A-Mater.* 2004, 78, 941-946.
9. Rowsell, J. L. C.; Eckert, J.; Yaghi, O. M., Characterization of H_2 Binding Sites in Prototypical Metal-Organic Frameworks by Inelastic Neutron Scattering. *J. Am. Chem. Soc.* 2005, 127, 14904-14910.

10. Brown, C. M.; Liu, Y.; Neumann, D. A., Neutron Powder Diffraction of Metal-Organic Frameworks for Hydrogen Storage. *Pramana J. Phys.* 2008, 71, 755-760.
11. Lee, H.; Choi, Y. N.; Choi, S. B.; Kim, J.; Kim, D.; Jung, D. H.; Park, Y. S.; Yoon, K. B., Liquid-Like Hydrogen Stored in Nanoporous Materials at 50 K Observed by in Situ Neutron Diffraction Experiments. *J. Phys. Chem. C* 2013, 117, 3177-3184.
12. Ramirez-Cuesta, A. J.; Jones, M. O.; David, W. I. F., Neutron Scattering and Hydrogen Storage. *Mater. Today* 2009, 12, 54-61.
13. Mitchell, P. C. H.; Parker, S. F.; Ramirez-Cuesta, A.; Tomkinson, J., Vibrational Spectroscopy With Neutrons : With Applications in Chemistry, Biology, Materials Science and Catalysis. World Scientific: Hackensack, NJ, 2005; P Xxvi, 642 P.
14. Gogotsi, Y.; Portet, C.; Osswald, S.; Simmons, J. M.; Yidirim, T.; Laudisio, G.; Fischer, J. E., Importance of Pore Size in High-Pressure Hydrogen Storage by Porous Carbons. *Int. J. Hydrogen Energ.* 2009, 34, 6314-6319.
15. Hruzewicz-Kołodziejczyk, A.; Ting, V. P.; Bimbo, N.; Mays, T. J., Improving Comparability of Hydrogen Storage Capacities of Nanoporous Materials. *Int. J. Hydrogen Energ.* 2011, 37, 2728-2736.
16. Silvera, I. F., the Solid Molecular Hydrogens in the Condensed Phase - Fundamentals and Static Properties. *Rev. Mod. Phys.* 1980, 52, 393-452.
17. Young, J. A.; Koppel, J. U., Slow Neutron Scattering by Molecular Hydrogen + Deuterium. *Phys Rev. A-Gen. Phys.* 1964, 135, A603
18. Colognesi, D.; Celli, M.; Ramirez-Cuesta, A. J.; Zoppi, M., Lattice Vibrations of Para-Hydrogen Impurities in a Solid Deuterium Matrix: An Inelastic Neutron Scattering Study. *Phys. Rev. B* 2007, 76, 174304.
19. Bimbo, N.; Ting, V. P.; Hruzewicz-Kołodziejczyk, A.; Mays, T. J., Analysis of Hydrogen Storage in Nanoporous Materials for Low Carbon Energy Applications. *Faraday Discuss.* 2011, 151, 59-74.
20. Sharpe, J. E.; Bimbo, N.; Ting, V. P.; Burrows, A. D.; Jiang, D.; Mays, T. J., Supercritical Hydrogen Adsorption in Nanostructured Solids With Hydrogen Density Variation in Pores. *Adsorption* 2013, 19, 643-652.
21. Tóth, J., Gas-(Dampf-) Adsorption An Festen Oberflachen Inhomogener Aktivitat .1. *Acta Chim. Hung.* 1962, 30, 415.
22. Dundar, E.; Zacharia, R.; Chahine, R.; Benard, P., Performance Comparison of Adsorption Isotherm Models for Supercritical Hydrogen Sorption on MOFs. *Fluid Phase Equilib.* 2014, 363, 74-85.
23. Liu, Y.; Kabbour, H.; Brown, C. M.; Neumann, D. A.; Ahn, C. C., Increasing the Density of Adsorbed Hydrogen With Coordinatively Unsaturated Metal Centers in Metal−Organic Frameworks. *Langmuir* 2008, 24, 4772-4777.
24. Yildirim, T.; Hartman, M. R., Direct Observation of Hydrogen Adsorption Sites and Nanocage Formation in Metal-Organic Frameworks. *Phys. Rev. Lett.* 2005, 95.
25. Luo, J.; Xu, H.; Liu, Y.; Zhao, Y.; Daemen, L. L.; Brown, C.; Timofeeva, T. V.; Ma, S.; Zhou, H.-C., Hydrogen Adsorption in a Highly Stable Porous Rare-Earth Metal-Organic Framework: Sorption Properties and Neutron Diffraction Studies. *J. Am. Chem. Soc.* 2008, 130, 9626-9327.
26. Ramirez-Cuesta, A. J.; Mitchell, P. C. H. Hydrogen Adsorption in a Copper ZSM5 Zeolite: An Inelastic Neutron Scattering Study *Catal. Today* 2007, 120, 368-373
27. Pigamo, A.; Besson, M.; Blanc, B.; Gallezot, P.; Blackburn, A.; Kozynchenko, O.; Tennison, S.; Crezee, E.; Kapteijn, F., Effect of Oxygen Functional Groups on Synthetic Carbons on Liquid Phase Oxidation of Cyclohexanone. *Carbon* 2002, 40, 1267–1278
28. Figueiredo, J. L.; Pereira, M. F. R.; Freitas, M. M. A.; Orfao J. J. M., Modification of the Surface Chemistry of Activated Carbons. *Carbon* 1999, 37,1379–1389
29. Zeiger, M.; Jäckel, N.; Aslan, M.; Weingarth, D.; Presser, V., Understanding Structure and Porosity of Nanodiamond-Derived Carbon Onions. *Carbon* 2015, 84, 584-598.
30. McDonough, J. K.; Frolov, A. I.; Presser, V.; Niu, J.; Miller, C. H.; Ubieto, T.; Fedorov, M. V.; Gogotsi, Y., Influence of the Structure of Carbon Onions on Their Electrochemical Performance in Supercapacitor Electrodes. *Carbon* 2012, 50, 3298-3309.

31 .Gogotsi, Y.; Dash, R. K.; Yushin, G.; Yildirim, T.; Laudisio, G.; Fischer, J. E., Tailoring of Nanoscale Porosity in Carbide-Derived Carbons for Hydrogen Storage. *J. Am. Chem. Soc.* 2005, 127, 16006-16007.
32. Yushin, G.; Dash, R.; Jagiello, J.; Fischer, J. E.; Gogotsi, Y., Carbide-Derived Carbons: Effect of Pore Size on Hydrogen Uptake and Heat of Adsorption. *Adv. Funct. Mater.* 2006, 16, 2288-2293.
33. Jagiello, J.; Anson, A.; Martinez, M. T., DFT-Based Prediction of High-Pressure H_2 Adsorption on Porous Carbons at Ambient Temperatures From Low-Pressure Adsorption Data Measured at 77 K. *J. Phys. Chem B* 2006, 110, 4531-4534.
34. Wang, Q. Y.; Johnson, J. K., Molecular Simulation of Hydrogen Adsorption in Single-Walled Carbon Nanotubes and Idealized Carbon Slit Pores. *J. Chem. Phys.* 1999, 110, 577-586.
35. Dundar, E.; Zacharia, R.; Chahine, R.; Bénard, P., Modified Potential Theory for Modeling Supercritical Gas Adsorption. *Int. J. Hydrogen Energ.* 2012, 37, 9137-9147.
36. Gallego, N. C.; He, L. L.; Saha, D.; Contescu, C. I.; Melnichenko, Y. B., Hydrogen Confinement in Carbon Nanopores: Extreme Densification at Ambient Temperature. *J. Am. Chem. Soc.* 2011, 133, 13794-13797.
37. Peterson, B. K.; Walton, J. P. R. B.; Gubbins, K. E., Fluid Behavior in Narrow Pores. *J. Chem. Soc. Farad. T. 2* 1986, 82, 1789-1800.
38. Brown, C. M.; Yildirim, T.; Neumann, D. A.; Heben, M. J.; Gennett, T.; Dillon, A. C.; Alleman, J. L.; Fischer, J. E., Quantum Rotation of Hydrogen in Single-Wall Carbon Nanotubes. *Chem. Phys. Lett.* 2000, 329, 311-316.
39. Ren, Y.; Price, D. L., Neutron Scattering Study of H_2 Adsorption in Single-Walled Carbon Nanotubes. *Appl. Phys. Lett.* 2001, 79, 3684-3686.
40. US Department of Energy, Explanations of Freedomcar/DOE Hydrogen Storage Technical Targets, Available From http://www1.eere.energy.gov/hydrogenandfuelcells//pdfs/freedomcar_targets_explanations.pdf.
41. Farha, O. K.; Yazaydin, A. O.; Eryazici, I.; Malliakas, C. D.; Hauser, B. G.; Kanatzidis, M. G.; Nguyen, S. T.; Snurr, R. Q.; Hupp, J. T., De Novo Synthesis of a Metal-Organic Framework Material Featuring Ultrahigh Surface Area and Gas Storage Capacities. *Nat. Chem.* 2010, 2, 944-948.

Additional references in Supplementary Information

42. Bimbo, N.; Sharpe, J. E.; Ting, V. P.; Noguera-Díaz, A.; Mays, T. J., Isosteric Enthalpies for Hydrogen Adsorbed on Nanoporous Materials at High Pressures. *Adsorption* 2013, 20, 373-384
43. Egelstaff, P. A.; Haywood, B. C.; Webb, F. J., Molecular Motions in Liquid and Solid Hydrogen and Deuterium. *Proc. Phys. Soc.* 1967, 90, 681.
44. Fitzgerald, S. A.; Yildirim, T.; Santodonato, L. J.; Neumann, D. A.; Copley, J. R. D.; Rush, J. J.; Trouw, F., Quantum Dynamics of Interstitial H_2 in Solid C_{60}. *Phys. Rev. B* 1999, 60, 6439-6451.
45. Celli, M.; Colognesi, D.; Zoppi, M., Direct Experimental Access to Microscopic Dynamics in Liquid Hydrogen. *Phys. Rev. E* 2002, 66.
46. Celli, M.; Colognesi, D.; Zoppi, M., Experimental Determination of the Translational Kinetic Energy of Liquid and Solid Hydrogen. *Eur. Phys. J. B* 2000, 14, 239-244.